Journal of Alloys and Compounds 522 (2012) 144–148

Contents lists available at SciVerse ScienceDirect

Journal of Alloys and Compounds

journal homepage: www.elsevier.com/locate/jallcom

Nanocrystalline $GaSbO_4$ with high surface area prepared via a facile hydrothermal method and its photocatalytic activity study

Yanghe Fu, Hun Xue, Meng Qin, Ping Liu, Xianzhi Fu, Zhaohui Li*

Research Institute of Photocatalysis, Fujian Provincial Key Laboratory of Photocatalysis – State Key Laboratory Breeding Base, Fuzhou University, Fuzhou 350002, PR China

ARTICLE INFO

Article history:
Received 3 November 2011
Received in revised form 20 January 2012
Accepted 23 January 2012
Available online 2 February 2012

Keywords:
Nanocrystalline materials
Hydrothermal
$GaSbO_4$
Salicylic acid
Acetone
Photocatalytic

ABSTRACT

Nanocrystalline $GaSbO_4$ with small particle size and large BET specific area was successfully prepared via a facile hydrothermal method from Sb_2O_5. The influence of the reaction pH on the formation of the final product was investigated. The obtained sample was characterized by X-ray diffraction (XRD), N_2-sorption BET surface area, UV–vis diffuse reflectance spectroscopy (DRS), transmission electron microscopy (TEM), high-resolution transmission electron microscopy (HRTEM). The photocatalytic activity for the degradations of salicylic acid and acetone over nanocrystalline $GaSbO_4$ under UV irradiations was for the first time revealed. Based on the electron spin resonance (ESR) result, the reactive species involved in the photocatalytic reaction over nanocrytalline $GaSbO_4$ are determined to be $HO^{\bullet}$ and $O_2^{-\bullet}$. The photocatalytic mechanism of $GaSbO_4$ was proposed.

1. Introduction

Semiconductor-based photocatalytic oxidation has been established to be one of the most promising technologies for the environment remediation and has been employed in the treatment of all kinds of organic contaminants [1–3]. The effective application of photocatalysis in environmental remediation requires that the photocatalysts should be of high photocatalytic efficiency. Therefore during the past decade, tremendous effort has been devoted to the development of new photocatalysts [4–11]. In addition to metal and non-metal ions doped TiO_2, single-phase-oxide-based photocatalysts consists of both d^0 and d^{10} central cations as well as a series of sulfides have been developed so far. However, some photocatalysts lack the long-term stability, while some show low activity, or require rigorous synthetic condition. The development of new photocatalysts with high performance is still a great challenge in photocatalysis so far.

Recently we and others have found that some metal oxides consist of central ion of Sb^{5+}, like $M_2Sb_2O_7$ ($M = Sr^{2+}$ and Ca^{2+}) [12–14], $PbSb_2O_6$ [15], $BiSbO_4$ [16,17] and $ZnSb_2O_6$ [18] show photocatalytic activity for the degradation of benzene and organic dyes. All these antimonate-based photocatalysts contain distorted Sb—O polyhedra and encourage us to explore the photocatalytic performance of other antimonates with distorted Sb—O polyhedra. $GaSbO_4$ crystallizes in the tetragonal structure with $P4_2/mnm$ space group and has a rutile-like structure. In its structure, Sb and Ga occupy the same position and the occupied probability is 0.5 for both Sb and Ga. The six-coordinated MO_6 octahedron is a compressed MO_6 octahedron with two shorter M—O bonds (1.951 Å) and four longer M—O bonds (1.999 Å). However, its application in the photocatalysis has never been explored previously. Besides this, most of the already reported antimonates are prepared by the conventional solid state reaction. It is generally known that the thus-prepared samples usually suffer from problems such as excessive crystal growth, small BET specific surface area, etc., which would lead to inferior photocatalytic activity. Recently we reported the synthesis of nanocrystalline $Sr_2Sb_2O_7$ [13] and $ZnSb_2O_6$ [18] with high specific area via a facile hydrothermal method using Sb_2O_5 as a starting material. It is therefore interesting to investigate whether such a facile method can be applied in the preparation of nanocrystalline $GaSbO_4$.

In this manuscript, we reported for the first time the facile synthesis of nanocrystalline $GaSbO_4$ with small particle size and large BET specific surface area from Sb_2O_5 via the hydrothermal method. The photocatalytic activity for the degradations of salicylic acid and gaseous acetone over the as-prepared nanocrystalline $GaSbO_4$ under UV irradiations was for the first time revealed and its photocatalytic mechanism was also proposed.

2. Experimental

2.1. Syntheses

All of the reagents were analytical grade and used without further purification. Nanocrystalline $GaSbO_4$ samples were prepared by a hydrothermal method

* Corresponding author. Tel.: +86 591 83779260; fax: +86 591 83779105.
E-mail address: zhaohuili1969@yahoo.com (Z. Li).

0925-8388/$ – see front matter © 2012 Elsevier B.V. All rights reserved.
doi:10.1016/j.jallcom.2012.01.141

using $Ga(NO_3)_3{\cdot}9H_2O$ and Sb_2O_5 as starting materials. In a typical procedure, Sb_2O_5 powder (0.4855 g, 1.5 mmol) were added to 8 ml aqueous solution containing $Ga(NO_3)_3{\cdot}9H_2O$ (1.2536 g, 3.0 mmol) under vigorous stirring. The pH of the resulting mixture was adjusted by nitric acid solution or sodium hydrate solution under vigorous stirring. The mixture was loaded into a 23 mL Teflon-lined autoclave, filled with de-ionized water up to 70% of the total volume and sealed tightly. Then the autoclaves were kept at 180 °C for 48 h. After cooling to room temperature, the precipitates were collected, washed with distilled water and absolute ethanol several times, and then dried in air at 80 °C (0.6521 g, 85%).

2.2. Characterizations

X-ray diffraction (XRD) patterns were collected on a Bruker D8 Advance X-ray diffractometer with CuK_α radiation. The accelerating voltage and the applied current were 40 KV and 40 mA, respectively. Data were recorded at a scanning rate of 0.004° $2\theta\,s^{-1}$ in the 2θ range of 10° to 70°. It was used to identify the phase present and their crystallite size. The crystallite size was calculated from X-ray line broadening analysis by Scherer equation: $D = 0.89\lambda/\beta\cos\theta$, where D is the crystal size in nm, λ is the CuK_α wavelength (0.15406 nm), β is the half-width of the peak in rad, and θ is the corresponding diffraction angle. UV–visible absorption spectra (UV-DRS) of the powders were obtained for the dry-pressed disk samples using a UV–visible spectrophotometer (Cary 500 Scan Spectrophotometers, Varian, USA). $BaSO_4$ was used as a reflectance standard in the UV–visible diffuse reflectance experiment. The transmission electron microscopy (TEM) and high resolution transmission electron microscopy (HRTEM) images were measured by JEOL model JEM 2010 EX instrument at the accelerating voltage of 200 kV. The powder particles were supported on a carbon film coated on a 3 mm diameter fine-mesh copper grid. A suspension of the sample in ethanol was sonicated and a drop was dripped on the support film. Electron spin resonance (ESR) spectra were obtained using Bruker model ESP 300 E electron paramagnetic resonance spectrometer.

2.3. Photocatalytic activity measurements

The photocatalytic activity of the as-prepared nanocrystalline $GaSbO_4$ was evaluated by the degradations of gaseous acetone and salicylic acid in an aqueous solution under UV irradiations. Photocatalytic degradation of salicylic acid was performed in a quartz tube with 4.7 cm inner diameter and 16.5 cm length. Four 4 W UV lamps with a wavelength centered at 254 nm (Philips, TUV 4 W/G4 T5) were used as illuminating source. 150 mg of $GaSbO_4$ were suspended in 150 mL of salicylic acid aqueous solution (5×10^{-4} mol/L) and stirred for 2 h before irradiation to ensure the reach of the adsorption/desorption equilibrium. A 4 mL aliquot was taken at 30 min intervals during the experiment and centrifuged (TDL-5-A). The resulting clear liquor was analyzed on a Varian UV–vis–NIR spectrophotometer (model: Cary-500). The percentage of degradation is reported as C/C_0. C is the absorption of salicylic acid at each irradiated time interval of the main peak of the absorption spectrum at wavelength 297 nm. C_0 is the absorption of the starting concentration when adsorption/desorption equilibrium was achieved.

The photocatalytic activity toward acetone was carried out in a 2500 mL glass container. The container was connected to a quartz reactor surrounded with four 4 W UV lamps (with major emission at 254 nm) and interfaced to a gas chromatograph (GC, Hewlett-Packard 4890). A closed circulation reaction system, including the container, the reactor and the GC, was established with the aid of a circulation pump. 0.30 g of the catalyst was packed into the quartz reactor with an inner size of 15 mm × 15 mm × 2 mm. Prior to the photodegradation experiments, the catalyst was allowed to reach a steady state with acetone in the dark for 4 h, and the equilibrium concentration of acetone was 350 ppm. The flow rate of the system was 20 mL/min, and the reaction temperature was controlled at 32 ± 1 °C by an air-cooling system. The concentrations of residual acetone and the produced CO_2 were measured at an interval of 20 min by gas chromatography, equipped with a Porapak R column, a flame ionization detector and a thermal conductivity detector.

3. Results and discussion

The XRD patterns of the resultant products through the hydrothermal process at 180 °C for 48 h under different pH values are shown in Fig. 1. It is observed that the pH value plays an important role in controlling the composition of the final products. For pH value was 1, pure $GaSbO_4$ (JCPDS: 480386) was obtained. When pH value was 3, the resultant product was a mixture of $GaSbO_4$ and GaOOH (JCPDS: 060180). When pH value was 8, Sb_6O_{13} started to appear and the resultant product was a mixture of $GaSbO_4$, GaOOH and Sb_6O_{13}. When pH value was raised to 12, only pure Sb_6O_{13} can be obtained. This indicates that pure $GaSbO_4$ can only be obtained under strong acidic condition when pH value is 1. The XRD patterns of the as-prepared $GaSbO_4$ samples show that the peaks are wide, indicating that the average crystallite sizes of the $GaSbO_4$ samples

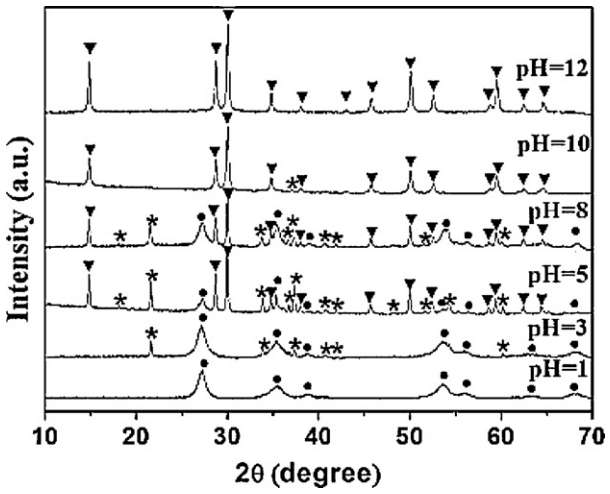

Fig. 1. XRD patterns of the samples prepared at 180 °C for 48 h with different pH: pH = 1; pH = 3; pH = 5; pH = 8; pH = 10; pH = 12. (●) $GaSbO_4$; (*) GaOOH; (▼) Sb_6O_{13}.

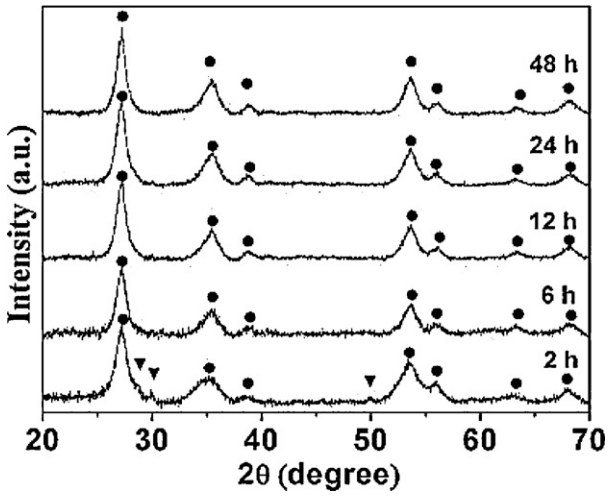

Fig. 2. XRD patterns of the samples prepared with pH = 1 at 180 °C for different time: 2 h; 6 h; 12 h; 24 h; 48 h. (●) $GaSbO_4$; (▼) Sb_6O_{13}.

are small. The average crystallite sizes calculated from the Scherrer equation are about 8 nm for the $GaSbO_4$ samples prepared when pH value is 1.

Unlike $Sr_2Sb_2O_7$, which can only be obtained under strong basic condition, pure $GaSbO_4$ can only be obtained under strong acidic condition. On the contrary, only Sb_6O_{13} can be obtained in strong basic condition. For a better understanding of the formation of nanocrystalline $GaSbO_4$, time-dependent experiments were carried out. It was found that a mixture of $GaSbO_4$ and Sb_6O_{13} were obtained when the reaction proceeded for only 2 h. This suggested that Sb_6O_{13} was an intermediate in this reaction. Pure $GaSbO_4$ was obtained when the hydrothermal time was longer than 6 h. With the increase of the hydrothermal time, the intensities of the diffraction peaks become stronger, indicating an enhanced crystallinity (Fig. 2).

Based on the time-dependent experiments, possible chemical reactions involved in the synthesis of $GaSbO_4$ nanoparticles can be formulated as the following:

$$Sb_2O_5 + H_2O \rightarrow 2SbO_3^- + 2H^+$$

$$6SbO_3^- + 6H^+ \leftrightarrow Sb_6O_{13} + 3H_2O + O_2$$

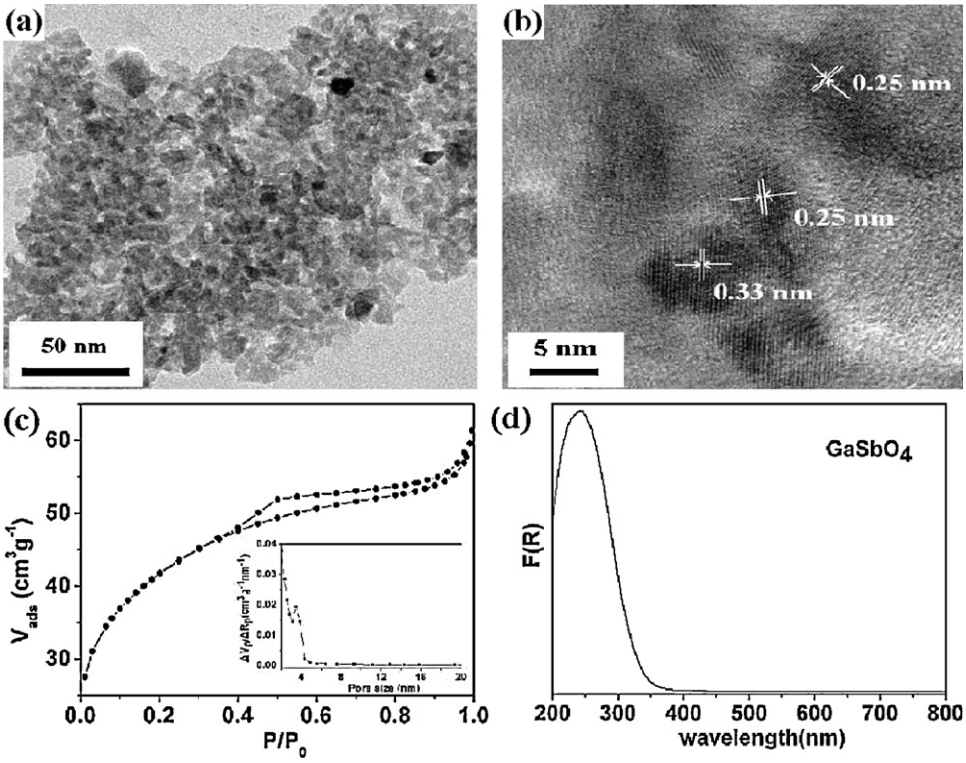

Fig. 3. $GaSbO_4$ sample prepared at 180 °C for 48 h under pH value of 1: (a) TEM image; (b) HRTEM Image; (c) nitrogen adsorption–desorption isotherm and the pore size distribution plot; (d) UV–vis diffuse reflectance absorption spectrum.

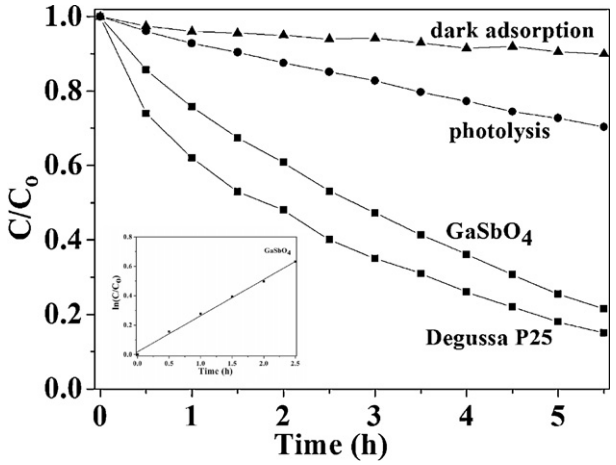

Fig. 4. Temporal changes of salicylic acid concentration as monitored by the UV–vis absorption spectra at 297 nm over $GaSbO_4$ with and without irradiations, pure UV irradiations and irradiated P25; inset: Pseudo-first-order plots of the degradation of salicylic acid over irradiated $GaSbO_4$.

$$SbO_3^- + Ga^{3+} + H_2O \rightarrow GaSbO_4 + 2H^+$$

In acidic condition, Sb_2O_5 is partly hydrolyzed to give SbO_3^- [19]. Anionic SbO_3^- could either react with Ga^{3+} to give $GaSbO_4$ nuclei or to undergo a self-redox reaction to give Sb_6O_{13}. The reaction between SbO_3^- and Ga^{3+} continues until all Sb_2O_5 and Sb_6O_{13} are consumed. The as-formed $GaSbO_4$ nuclei grow to form $GaSbO_4$ nanoparticles. On the contrary, under basic condition, Sb_2O_5 is partly hydrolyzed to give $Sb(OH)_6^-$ and Ga^{3+} is hydrolyzed to give $Ga(OH)_4^-$. [20] It would be difficult for the anionic $Ga(OH)_4^-$ to react with the anionic $Sb(OH)_6^-$. Therefore it is not able to obtain $GaSbO_4$ nanoparticles in high pH value.

The TEM image of $GaSbO_4$ prepared at 180 °C for 48 h under pH value of 1 show that the sample consists entirely of small particles with the average size at around 8 nm, which is consistent with the result from XRD according to the Scherrer formula (Fig. 3a). Clear lattice fringes of $d = 0.25$ nm and $d = 0.33$ nm, which match that of the (1 0 1) and (1 1 0) plane of $GaSbO_4$ respectively, can be observed in HRTEM image (Fig. 3b). The EDS indicates the presence of Ga, Sb and O and the atomic ratio of Ga and Sb is about stoichiometry 1:1 and indicates that no impurity exists. The N_2-sorption isotherm (Fig. 3c) for the hydrothermal prepared $GaSbO_4$ exhibits stepwise adsorption and desorption (type IV isotherm), indicative of a mesoporous solid. The average pore size for $GaSbO_4$ is about 3.0 nm with a narrow distribution of pore size. This porosity is originated from the inter-particle porosity. As compared with other antimonate-based photocatalysts like $Sr_2Sb_2O_7$ (29.8 m^2/g) [13] and $BiSbO_4$ (18.3 m^2/g) [17] prepared via a similar hydrothermal method, the

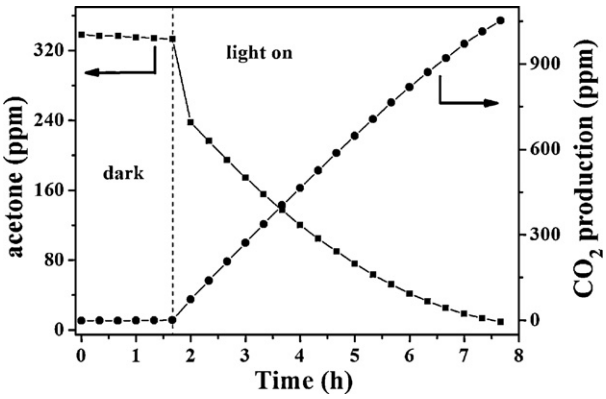

Fig. 5. The conversion of acetone and the amount of produced CO_2 over $GaSbO_4$ as a function of reaction time. (■) the conversion of acetone over $GaSbO_4$; (●) the amount of produced CO_2 over $GaSbO_4$.

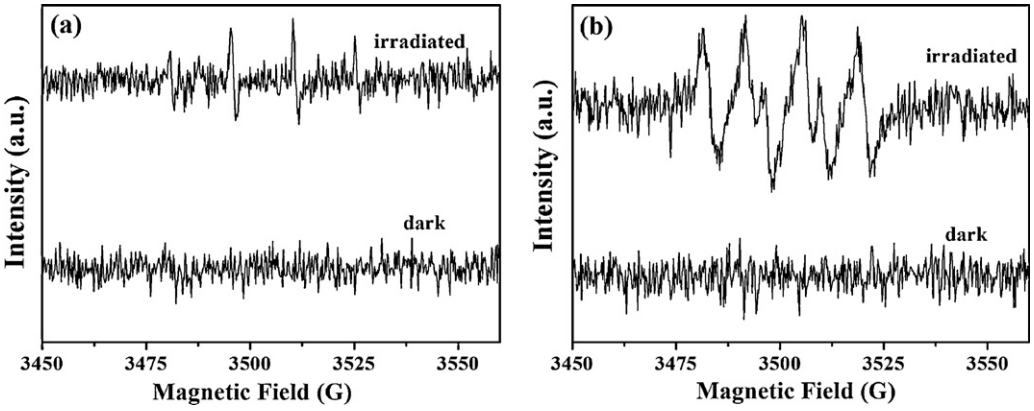

Fig. 6. DMPO spin-trapping ESR spectra over $GaSbO_4$ prepared at 180 °C for 48 h under pH value of 1 (a) in aqueous dispersion for DMPO-•OH; (b) in methanol dispersion for DMPO-$O_2^{-\bullet}$.

as-prepared $GaSbO_4$ shows a very high BET specific surface area of 130.0 m^2/g. It indicates that the hydrothermal method is an efficient method to prepare nanocrystalline $GaSbO_4$ with small particle size and large BET specific surface. The UV–vis DRS spectrum of the as-prepared $GaSbO_4$ shows that the absorption edge locates at ca. 335 nm, corresponding to a band gap of about 3.7 eV (Fig. 3d).

The photocatalytic activity of the as-prepared $GaSbO_4$ was evaluated by the degradation of salicylic acid in the aqueous solution. Temporal changes in the concentration of salicylic acid were monitored by examining the variations in the maximal absorption in UV–vis spectra at 297 nm. Fig. 4 shows the results of the degradation of salicylic acid in the presence of $GaSbO_4$. After 5.5 h irradiations, only about 25% of salicylic acid was degraded under pure UV irradiations, while about 80% of salicyclic acid was converted over nanocrystalline $GaSbO_4$. The conversion ratio over irradiated $GaSbO_4$ is comparable to that observed over commercial Degussa P25 (85%), indicating that $GaSbO_4$ is an active photocatalyst.

To quantitatively understand the reaction kinetics of the salicylic acid degradation in our experiments, we applied the pseudo-first order model as expressed by Eq. (1), which is generally used for photocatalytic degradation process if the initial concentration of pollutant is low:

$$\ln\left(\frac{C_0}{C}\right) = kt \quad (1)$$

where C_0 is the initial concentration, C is the concentration after a time (t) of the salicylic acid degradation, and k is the first-order rate constant. It is clear that a fairly good correlation to the pseudo-first order reaction kinetics is found (Fig. 4 inset). The determined reaction rate constant k for salicylic acid degradation is 0.26947 h^{-1}.

$GaSbO_4$ also shows photocatalytic activity for the degradation of gaseous acetone under UV irradiations. The concentration change of acetone and CO_2 in the system as a function of UV irradiations time was shown in Fig. 5. Within 6 h illuminations, about 96% of the initial CH_3COCH_3 (350 ppm) was degraded and almost 100% of the degraded CH_3COCH_3 was mineralized to CO_2 (1010 ppm) over $GaSbO_4$.

The observation of photocatalytic activity for the degradation of salicylic acid and acetone over $GaSbO_4$ again confirms that antimonates contain distorted Sb—O polyhedron in their structure can be promising photocatalyst. Usually the reactive species involved in the photocatalytic reactions over semiconductor photocatalysts are believed to be oxygen radicals like $O_2^{-\bullet}$ and OH•. To generate these reactive radicals, the semiconductor photocatalyst should have appropriate band structure, so that the photogenerated charge carriers have strong enough redox abilities. Based on Butler semi-empirical formula $E_{CB} = X - E_c - 0.5E_g$ [21], the edge of the conduction band (E_{CB}) of $GaSbO_4$ is estimated to be −0.36 V (vs. NHE), while the edge of the valence band (E_{VB}) is calculated to be 3.34 V (vs. NHE). Since the conduction band is more negative than that of $E^\circ(O_2/O_2^{-\bullet})$ (−0.33 V vs. NHE), and the valence band (E_{VB}) is positive than that of $E^\circ(OH^\bullet/OH^-)$ (2.38 V vs. NHE), it is suggested that the photogenerated holes over $GaSbO_4$ can oxidize OH^- to give $OH^\bullet$, while the photogenerated electrons can reduce O_2 to give $O_2^{-\bullet}$ [22]. The generation of both $HO^\bullet$ and $O_2^{-\bullet}$ over illuminated $GaSbO_4$ is confirmed by the ESR results (Fig. 6a and b). Capable of producing highly reactive $HO^\bullet$ and $O_2^{-\bullet}$ radicals can explain the photocatalytic activity of $GaSbO_4$.

4. Conclusions

In summary, nanocrystalline $GaSbO_4$ with large specific surface area has been prepared by a facile hydrothermal method directly from Sb_2O_5. The as-prepared nanocrystalline $GaSbO_4$ showed photocatalytic activity for the degradations of aqueous salicylic acid and gaseous acetone. The preparations of other ternary antimonates and the investigations of their photocatalytic activity are still going on in our laboratory.

Acknowledgements

The work was supported by National Natural Science Foundation of China (20977016, U1033603), National Basic Research Program of China (973 Program: 2010CB234604) and Program for Changjiang Scholars and Innovative Research Team in University (PCSIRT0818). The Award Program for Minjiang Scholar Professorship and the NSF of Fujian province for Distinguished Young Investigator Grant (2009J06004) to Z. Li are also acknowledged.

References

[1] M.R. Hoffmann, S.T. Martin, W. Choi, D.W. Bahnemann, Chem. Rev. 95 (1995) 69–96.
[2] A. Fujishima, T.N. Rao, D.A. Tryk, J. Photochem. Photobiol. C 1 (2000) 1–21.
[3] C.C. Chen, W.H. Ma, J.C. Zhao, Chem. Soc. Rev. 39 (2010) 4206–4219.
[4] S.X. Ouyang, J.H. Ye, J. Am. Chem. Soc. 133 (2011) 7757–7763.
[5] Z.H. Ai, L.Z. Zhang, S.C. Lee, J. Phys. Chem. C 114 (2010) 18594–18600.
[6] J.G. Yu, G.P. Dai, B.B. Huang, J. Phys. Chem. C 113 (2009) 16394–16401.
[7] H.F. Shi, Z.S. Li, J.H. Kou, J.H. Ye, Z.G. Zou, J. Phys. Chem. C 115 (2011) 145–157.
[8] S. Zhu, T. Xu, H. Fu, J. Zhao, Y. Zhu, Environ. Sci. Technol. 41 (2007) 6234–6239.
[9] Y. Bi, S. Ouyang, J. Cao, J. Ye, Phys. Chem. Chem. Phys. 13 (2011) 10071–10075.
[10] F.Q. Huang, J.j. Wu, X.P. Lin, Z. Zhou, J. Alloys Compd. 509 (2011) 764–768.
[11] X.L. Huang, J. Lv, Z.S. Li, Z.G. Zou, J. Alloys Compd. 507 (2010) 341–344.
[12] X.P. Lin, F.Q. Huang, W.D. Wang, Y.M. Wang, Y.J. Xia, J.L. Shi, Appl. Catal. A: Gen. 313 (2006) 213–218.
[13] H. Xue, Z.H. Li, L. Wu, Z.X. Ding, X.X. Wang, X.Z. Fu, J. Phys. Chem. C 112 (2008) 5850–5855.

[14] X. Lin, J. Wu, X. Lv, Z. Shan, W. Wang, F. Huang, Phys. Chem. Chem. Phys. 11 (2009) 10047–10052.
[15] K.L. Zhang, X.P. Lin, F.Q. Huang, Y.M. Wang, J. Mol. Catal. A: Chem. 258 (2006) 185–190.
[16] X.P. Lin, F.Q. Huang, W.D. Wang, K.L. Zhang, Appl. Catal. A: Gen. 307 (2006) 257–262.
[17] Q.Q. You, Y.H. Fu, Z.X. Ding, L. Wu, X. Wang, Z.H. Li, Dalton Trans. 40 (2011) 5774–5780.
[18] W.J. Liu, P.Y. Lin, H. Jin, H. Xue, Y.F. Zhang, Z.H. Li, J. Mol. Catal. A: Chem. 349 (2011) 80–85.
[19] S.H. Gate, E. Richardson, J. Inorg. Nucl. Chem. 23 (1961) 257–263.
[20] W. Sheets, E. Mugnier, A. Barnabé, T. Marks, K. Poeppelmeier, Chem. Mater. 18 (2006) 7–20.
[21] M.A. Butler, D.S. Ginley, J. Electrochem. Soc. 125 (1978) 228–232.
[22] A.J. Bard, R. Parsons, J. Jordan, Standard Potentials in Aqueous Solution, Marcel Dekker, New York and Basel, 1985.